2014 International Joint Conference on Neural Networks (IJCNN)
July 6-11, 2014, Beijing, China

Ultra-Short-Pulse Acoustic Imaging Using Complex-Valued Spatio-Temporal Neural-Network for Null-Steering: Experimental Results

Kotaro Terabayashi and Akira Hirose

***Abstract*—This paper reports experimental results of a wide-band acoustic imaging method based on power-inversion adaptive array (PIAA) scheme realized by a complex-valued spatio-temporal neural network (CVSTNN). For acoustic imaging with a high resolution in the range direction (direction of propagation), used pulse should be short. A short pulse has a wide frequency band, which is also favorable for avoidance of target breaking through acoustic resonance. However, because of the wide bandwidth, conventional adaptive arrays often fail in beamforming or null steering. We combine a CVSTNN and PIAA to realize a precise null steering. Experiments demonstrate that the CVSTNN-PIAA method presents a higher resolution than conventional methods.**

I. Introduction

ACOUSTIC imaging is a technology widely used in various fields such as health diagnosis and non-destructive inspection. It is often used under water and/or inside materials in which optical techniques is unavailable. In the future, local precise observation inside the human body such as stomach and intestines walls or concrete interspaces will also become possible if a small sensor is applicable in combination with endoscope surface observation and/or sensor capsules.

In usual human body imaging, a high frequency ultrasonic wave is transmitted from wide aperture sensor elements. Electronic switching of the elements realizes beam scanning for imaging. This method cannot acquire images for a low-frequency low-loss scattering observation and/or with a use of small aperture sensor elements to be inserted into small space because of a large diffraction phenomenon.

Another scanning method is electronic adaptive beamforming using a sensor array. There exist several beamforming techniques. The most basic one is the delay and sum (DAS) method. The so-called Capon's method [1] is also a widely used beamforming and imaging technique to realize a sharp beam as a main lobe with suppression of side lobes [2], [3], [4]. DAS and Capon's methods obtain images by scanning the beam. Instead, another imaging is also possible by employing super-resolution techniques such as the MUSIC [5] and ESPRIT [6] algorithms often with a higher angle resolution. In these schemes, null points, i.e., very low-sensitive direction points among lobes in the radiation pattern (sensitivity pattern), are scanned around. Since a null is

The authors are with the Department of Electrical Engineering and Information Systems, The University of Tokyo, Tokyo 113-8656, Japan. e-mail: (see http://www.eis.t.u-tokyo.ac.jp). This work was partly supported by JSPS KAKENHI Grant Number 18360162.

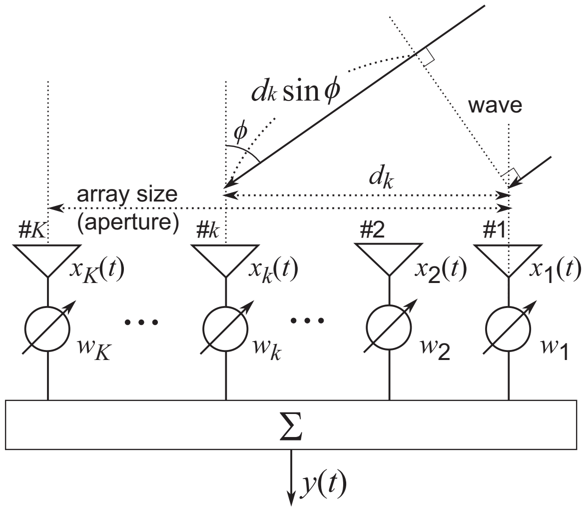

Fig. 1. Linear sensor array corresponding to conventional delay-and-sum (DAS) scheme with definition of basic array-configuration parameters.

generally sharper than a beam, we can achieve a resolution higher than that in normal beamforming.

In all the methods mentioned above, however, the steering angle depends on the wavelength of the acoustic wave. Then the frequency bandwidth of the transmitted wave has to be narrow enough to realize a fine alignment of the wavefront. A narrow band wave pulse possesses a long wave packet, and requires some special technique to obtain a high resolution in the range direction, i.e., direction along the propagation, for local precise observation [7] [8] [9]. A narrow band wave can also cause breaking of target objects through acoustic resonance.

Previously, we proposed a wideband beamforming method based on a complex-valued spatio-temporal neural network (CVSTNN) combined with power-inversion adaptive array (PIAA) [10]. A wideband system has low energy density in the frequency spectrum and, hence, it is less invasive. The short pulse leads to a higher range resolution and less speckle noise. Simulation results showed that the resolution of the CVSTNN-PIAA method can be very high.

In this paper, we present preliminary imaging results of the CVSTNN-PIAA method showing a high resolution in azimuth direction with a very short pulse. Though, in practice, ultrasound transducer often shows a non-negligible nonlinearity and distortion, the experimental results promise the future development of ultra-short-pulse acoustic imaging

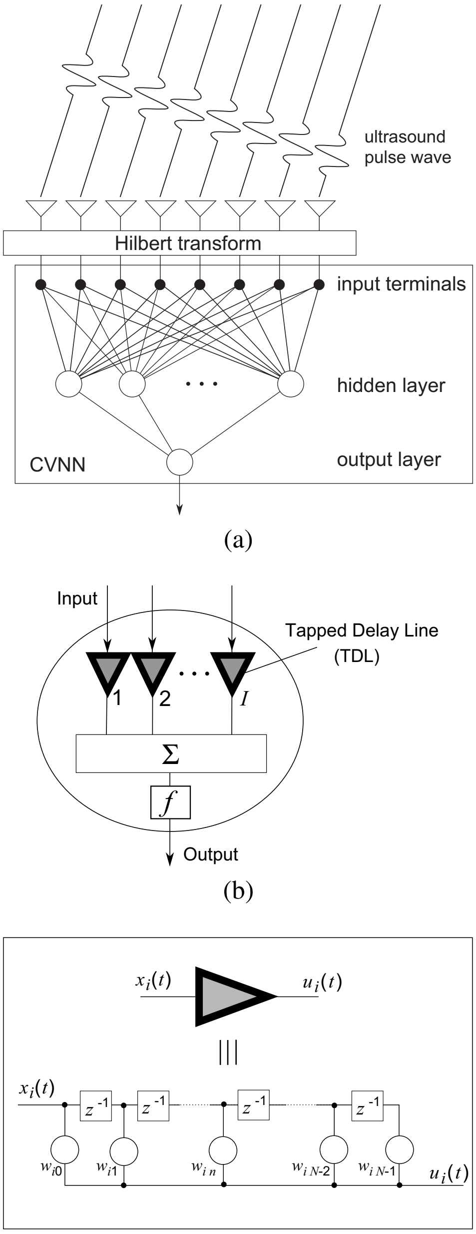

Fig. 2. Complex-valued neural network to realize beamforming of ultra wideband signals (a) basic construction of CVSTNN, (b) neuron structure, and (c) tapped delay line (TDL).

in various fields.

II. Imaging Based on Complex-Valued Spatio-Temporal Neural Networks

A. Imaging Process Based on Complex-Valued Spatio-Temporal Neural Network Power-Inversion Adaptive Array (CVSTNN-PIAA)

We present the construction and dynamics of an acoustic imaging method consisting of a complex-valued spatio-temporal neural network (CVSTNN) [11] and the power-inversion adaptive array (PIAA) technique [12]. In this paper, we assume discrete target objects, and realize the imaging by steering nulls to the targets to estimate the direction of arrival (DoA) for imaging.

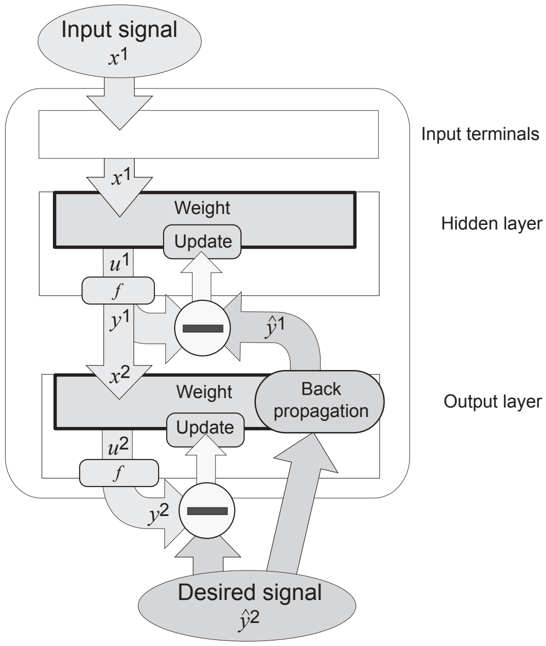

Fig. 3. Complex-valued backpropagation learning.

Fig. 1 shows the basic construction of the one-dimensional sensor array. Let us consider M discrete urtrasonic scatterers (targets) in space. Ultrasound is transmitted to the space, scattered at the targets, and received at the sensor array. Each sensor generate time-sequential M pulses at maximum. We estimate the DoA based on the obtained time-sequential signals for the multiple scatterers to generate a scatterers image.

We train the CVSTNN to direct its nulls to the estimated DoA of the M pulses. The learning is realized by feeding to the CVSTNN the received signals as teacher input signals while constant zeros as a teacher output signal. Then the nulls are directed to the pulse arrival directions. Next we calculate the radiation pattern (directional sensitivity) of the array by generating, feeding and steering a formal pulse numerically within the CVSTNN. The peaks in the inverse of the radiation pattern show the estimation of the target directions, which is equivalent to a scatterer space image.

B. Learning Dynamics of Complex-Valued Neural Network

1) Construction: This section presents its construction and the learning process to be used in the imaging system mentioned in the previous section [11]. Fig.2 shows the construction of the CVSTNN consisting of an input terminal layer, a hidden neuron layer and an output neuron layer. Signals detected at the sensors are converted into analytical signals by Hilbert transform which makes the phase values of positive- and negative-frequency components advance and retardant by $\pi/2$ rad, respectively. The analytical signal is expressed by the Hilbert transform $\mathcal{H}$ and received signals $\boldsymbol{x}$ as $(1 + j\mathcal{H})\,\boldsymbol{x}$. It is fed to and processed by the CVSTNN.

Fig.2(b) illustrates the inside of a neuron. The signals run through tapped delay lines (TDLs) which work as synaptic weights. Then they are summed up to become the neural internal state u, and finally to generate a neural output in the range of $[-1, 1]$ as $f(u) = \tanh(|u|)\exp(i \arg(u))$ where $f(u)$ is an activation function.

Fig.2(c) presents the structure of the TDL working as a synaptic weight. The z^{-1} box stands for a unit delay, and $w_{in} = a_{in} \exp(j\theta_{in})$ is a weight at the n-th tap for i-th input. The output of the TDL is the weighted sum of the time-sequential signals existing in the delay line, and generate the internal state u, as

$$u_i(t) = \sum_{n=0}^{N-1} x_i(t-n) w_{in} \tag{1}$$

$$u(t) = \sum_i u_i(t) \tag{2}$$

The CVSTNN realizes an adaptive beamformer for wideband signals in combination with the sensor array by adjusting the amplitude and phase values of the TDL weights $w(n)$ through complex-valued neural learning mentioned below.

2) Learning Dynamics: The learning dynamics is explained as follows [13] [14] [15]. The outline is shown in Fig.3. First we prepare a set of teacher signals as combinations of input signals and corresponding desired output signals for the supervised learning. The input signals propagate forward to generate output, whereas the teacher output signals propagate backward to the input. In this learning, the teacher signals themselves, instead of errors, backpropagate through the network [16] [17] [18] . The teacher signals $\hat{y}^{l-1}$ in layer $l-1$ is given by the teacher signals $\hat{\boldsymbol{y}}^l = [\hat{y}_j^l]^T \equiv [|\hat{y}_j^l| \exp\{j\hat{\theta}_j^l\}]^T$ and weights $\mathbf{W}^l = [\boldsymbol{w}_1^l \ldots \boldsymbol{w}_j^l \ldots \boldsymbol{w}_J^l]$ for $\boldsymbol{w}_j^l \equiv [w_{jin}^l]$ at n-th tap i-th input of j-th neuron in layer l as

$$\hat{\boldsymbol{y}}^{l-1} = (f(\ (\hat{\boldsymbol{y}}^l)^* \ \mathbf{V}^l \ ))^* \tag{3}$$

where $\mathbf{V}^l = [v_{jin}]^l \equiv w_{jin}^l / |w_{jin}^l|^2$. Each neuron calculates the difference of the temporary output and the backpropagating teacher signal, and changes the weights according to the difference as [13]

$$\begin{aligned} |w_{jin}|^{\mathrm{new}} &= |w_{jin}|^{\mathrm{old}} - K\Big\{ \left(1 - |y_j|^2\right) \\ &\quad \Big(|y_j| - |\hat{y}_j| \cos\Big(\theta_j - \hat{\theta}_j\Big)\Big) |x_{in}| \cos\theta_{jin}^{\mathrm{rot}} \\ &\quad - |y_j||\hat{y}_j| \sin\Big(\theta_j - \hat{\theta}_j\Big) \frac{|x_{in}|}{|u_j|} \sin\theta_{jin}^{\mathrm{rot}} \Big\} \end{aligned} \tag{4}$$

$$\begin{aligned} \theta_{jin}^{\mathrm{new}} &= \theta_{jin}^{\mathrm{old}} - K\Big\{ \left(1 - |y_j|^2\right) \\ &\quad \Big(|y_j| - |\hat{y}_j| \cos\Big(\theta_j - \hat{\theta}_j\Big)\Big) |x_{in}| \sin\theta_{jin}^{\mathrm{rot}} \\ &\quad + |y_j||\hat{y}_j| \sin\Big(\theta_j - \hat{\theta}_j\Big) \frac{|x_{in}|}{|u_j|} \cos\theta_{jin}^{\mathrm{rot}} \Big\} \end{aligned} \tag{5}$$

where $w_{jin} \equiv |w_{jin}| \exp\{\theta_{jin}\}$ (layer index l is omitted), $(\cdot)^{\mathrm{new}}$ and $(\cdot)^{\mathrm{old}}$ stand for update from old to new, $\theta_{jin} \equiv \arg(w_{jin})$, $\theta_j \equiv \arg(y_j)$ and $\theta_{jin}^{\mathrm{rot}} \equiv \theta_j - \theta_i - \theta_{jin}$.

TABLE I
EXPERIMENTAL SETUP AND NEURAL PARAMETERS.

Setup / Parameter			Value	
Number of scatterers			3	
Direction & distance	ϕ_1=0,	ψ_1=0 [deg],	225	[mm]
	ϕ_2=9.3,	ψ_2=0 [deg],	251	[mm]
	ϕ_3=14.9,	ψ_3=0 [deg],	233	[mm]
Pulse center frequency			500	[kHz]
Fractional bandwidth			0.74	
Sampling frequency			10	[MHz]
Number of sensors			8×8	(2 dim.)
Array pitch			2.0	[mm]
Array size			14.0	[mm]

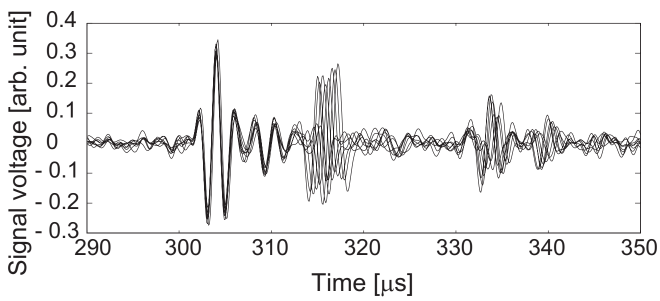

Fig. 4. Example of observed waveforms in time domain showing the response of 8 sensors aligned one-dimensionally in a line through the array center.

The formulation is derived in complex-valued neural networks employing amplitude-phase-type complex nonlinearity as the neural activation function, which is one of the widely used complex-valued network dynamics. In the iteration of the above learning process, the CVSTNN changes the output in such a way that the temporary output $\boldsymbol{y}^l$ converges at the desired one $\hat{\boldsymbol{y}}^l$ with appropriate (phase–amplitude focused) generalization characteristics arising from the complex-valued learning dynamics. The adaptive antenna system in total learns nulls for a set of teacher signals, namely, teacher input signals of incident pulses from arbitrary directions ϕ and an output signal of zero (no output), or learns to direct a beam to arbitrary directions ϕ with a pulse output teacher signal.

In the null learning, we have to avoid the trivial solution $\mathbf{W}^1 = \mathbf{0}$. For this purpose, we choose one connection in each neural layer, and replace the adaptive TDL of the connection with a direct connection, through which the signals pass without modification [10]. Then the learning realizes the cancel of the signals passing through the direct connections, resulting in the avoidance of the trivial solution.

III. Underwater Experiment Evaluation of Imaging Performance

A. Experimental setup

We report experimental results conducted under water. We use an 8×8 two-dimensional sensor array. The array size is very small (14×14 mm^2). We prepared three targets of expanded polystyrene shaped as spheres of 1 cm diameter. The three scatterers are placed in 0-deg, 9.3-deg and 14.9-deg

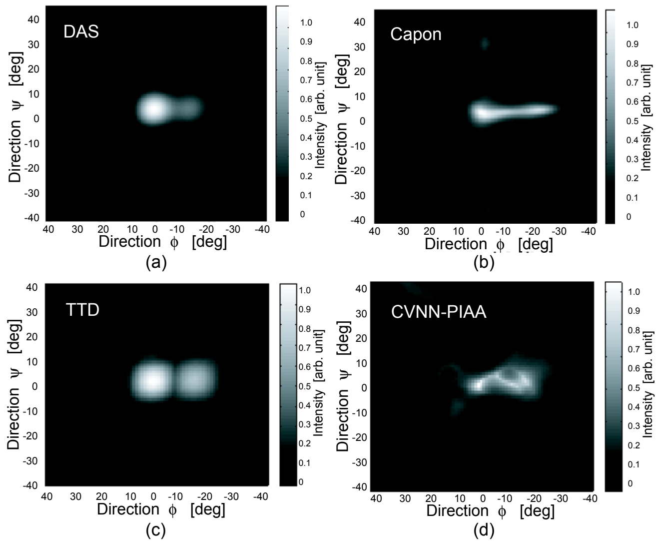

Fig. 5. Experimental two-dimensional imaging results for (1)DAS, (2)CAPON, (3)TTD and proposed CVSTNN-PIAA methods.

ϕ-directions with different distances of 225 mm, 221 mm and 233 mm, respectively. Experimental and neural parameters are shown in Table I.

Fig.4 shows an example of signal sets detected by the 8 linear array sensors, among the 64 sensors, aligned one-dimensionally on a line through the two-dimensional array center. Since the pulse is very short, the waveform becomes a summation of sharp pulses in total. Note that all the sensor elements can also work as transmitter elements. In this experiment, we chose one element at the center as the transmitter, and used all the elements as the receivers. The three target signals exist in the region of $t =$290–350 μs. We aim the imaging of this region by estimating the DoA for the three targets simultaneously.

B. Imaging results

Fig.5 presents the imaging results for the DAS, Capon's, TTD and CVSTNN-PIAA methods. Here ψ stands for the direction perpendicular to ϕ. Despite the closeness of the 9.3-deg and 14.9-deg targets and the smallness of the array size of 14×14 mm^2 for the low frequency of 500kHz, we can nearly distinguish them successfully in the CVSTNN-PIAA method. The image is somewhat distorted, which is a problem to be mitigated possibly by analyzing also frequency-domain generalization ability [19]. In other methods, however, they are not separate. The resulted images show the high resolution of the proposed CVSTNN-PIAA method.

IV. Conclusion

We presented the experimental results of a wideband acoustic imaging method using a complex-valued spatio-temporal neural network (CVSTNN). We combined the CVSTNN and power-inversion adaptive array (PIAA) to realize a high-resolution null learning even for very short pulses and small-aperture array. The results of the underwater experiments demonstrated that the CVSTNN-PIAA method shows a higher resolution than the conventional DAS, Capon or TTD methods. This adaptive method will be useful also in electromagnetic-wave imaging which often suffers from direct coupling among antenna elements.

References

[1] J. Capon, "High-resolution frequency-wavenumber spectrum analysis," *Proceedings of the IEEE*, vol. 57, no. 8, pp. 1408–1418, 1969.
[2] Z. Wang, J. Li, P. Stoica, T. Nishida, and M. Sheplak, "Constant-beamwidth and constant-powerwidth wideband robust capon beamformers for acoustic imaging," *Journal of the Acoustical Society of America*, vol. 116, pp. 1621–1631, 2004.
[3] I. Holfort, F. Gran, and J. Jensen, "P2b-12 minimum variance beamforming for high frame-rate ultrasound imaging," in *IEEE Ultrasonics Symposium, 2007.*, oct. 2007, pp. 1541 –1544.
[4] J.-F. Synnevag, A. Austeng, and S. Holm, "Benefits of minimum-variance beamforming in medical ultrasound imaging," *IEEE Transactions on Ultrasonics, Ferroelectrics and Frequency Control*, vol. 56, no. 9, pp. 1868 –1879, september 2009.
[5] R. Schmidt, "Multiple emitter location and signal parameter estimation," *IEEE Transactions on Antennas and Propagation*, vol. 34, no. 3, pp. 276 – 280, mar 1986.
[6] R. Roy and T. Kailath, "Esprit-estimation of signal parameters via rotational invariance techniques," *IEEE Transactions on Acoustics, Speech and Signal Processing*, vol. 37, no. 7, pp. 984 –995, 1989.
[7] T. Nishino, R. Yamaki, and A. Hirose, "Phase singular point elimination in ultrasonic images based on complex-valued markov random field model," in *Symposium on Ultrasonic Electronics (USE) 2008 Tsukuba*, no. 3-02P-11, November 2007.
[8] T. Nishino, M. Ueki, and A. Hirose, "Adaptive beamforming in superdirectional acoustic systems," in *Symposium on Ultrasonic Electronics (USE) 2008 Tsukuba*, 2007.
[9] T. Nishino, R. Yamaki, and A. Hirose, "Ultrasonic imaging for boundary shape generation by phase unwrapping with singular-point elimination based on complex-valued Markov random field model," *IEICE Transactions on Fundamentals*, vol. E93-A, no. 1, pp. 219–226, January 2010.
[10] K. Terabayashi and A. Hirose, "Proposal of ultra-short-pulse acoustic imaging using complex-valued spatio-temporal neural-network null-steering," in *Proceedings of International Conference on Neural Information Processing (ICONIP) 2013 Daegu*, no. III, November 2013, pp. 217–224.
[11] A. B. Suksmono and A. Hirose, "Beamforming of ultra-wideband pulses by a complex-valued spatio-temporal multilayer neural network," *International Journal of Neural Systems*, vol. 15, no. 1, pp. 1–7, 2005.
[12] R. Compton, "The power-inversion adaptive array: Concept and performance," *IEEE Transactions on Aerospace and Electronic Systems*, vol. AES-15, no. 6, pp. 803 –814, nov. 1979.
[13] A. Hirose and S. Yoshida, "Generalization characteristics of complex-valued feedforward neural networks in relation to signal coherence," *IEEE Transactions on Neural Networks and Learning Systems*, vol. 23, pp. 541–551, 2012.
[14] A. Hirose, *Complex-Valued Neural Networks, 2nd Edition.* Heidelberg, Berline, New York: Springer, 2012.
[15] A. Hirose (Ed.), *Complex-Valued Neural Networks: Advances and Applications*, ser. IEEE Press Series on Computational Intelligence. New Jersey, U.S.A.: IEEE Press and Wiley, April 2013.
[16] A. Hirose, "Applications of complex-valued neural networks to coherent optical computing using phase-sensitive detection scheme," *Information Sciences –Applications–*, vol. 2, pp. 103–117, 1994.
[17] A. Hirose and R. Eckmiller, "Behavior control of coherent-type neural networks by carrier-frequency modulation," *IEEE Transactions on Neural Networks*, vol. 7, pp. 1032–1034, 1996.
[18] S. Kawata and A. Hirose, "A coherent optical neural network that learns desirable phase values in frequency domain by using multiple optical-path differences," *Optics Letters*, vol. 28, no. 24, pp. 2524–2526, 2003.
[19] ——, "Frequency-multiplexed logic circuit based on a coherent optical neural network," *Applied Optics*, vol. 44, no. 19, pp. 4053–4059, 2005.